Sound Absorption of a Baffled Cavity-backed Micro-perforated Panel Absorber under Oblique and Diffused Incidence

Cheng YANG* and Li CHENG*,^
*Department of Mechanical Engineering, The Hong Kong Polytechnic University
Hung Hom, Kowloon, Hong Kong, SAR of China
^E-mail: mmlcheng@polyu.edu.hk

Abstract

The sound absorption performance of an absorber composed of a baffled micro-perforated panel (MPP) backed by a cavity is investigated in this paper. As a continuation of our previous work focusing on the normal incidence case, a three dimensional model is established which allows the consideration of oblique and diffused sound impingement on an absorber of finite dimension. The extreme case having a large panel dimension is used to approximate an absorber of infinite dimension, which is compared numerically with Maa's formula to show the validity of the model. It is observed that the grazing modes of the backing cavity can be efficiently excited under the grazing incidence. These grazing modes contribute significantly to the total sound absorption, which contrasts with the case of normal incidence. Analysis shows the underlying physics of the sound absorption based on modal coupling, which differs significantly when incident angle varies. Hence for an absorber in a diffused field, multiple modes would dominate the sound absorption, leaving large rooms for optimal design of the absorber towards better absorption performance.

Key words: MPP, oblique incidence, vibro-acoustic coupling

1. Introduction

The micro-perforated panel (MPP) is an efficient tool for noise abatement. Initially proposed by Maa [1], a MPP consists of a sheet panel with a lattice of sub-millimeter size perforation distributed over its surface. The use of MPP absorber in various configurations for the noise abatement has been investigated by many researchers. Li *et al* [2] studied the influence of the structure vibration to the performance of the MPP absorber and it was found that the panel vibration effect could widen the effective absorption band. A thick MPP which aims to enhance the strength of the device for practical use was studied by Sakagami *et al* [3]. And it was observed that the MPP is potentially efficient if a tapered profile was applied at the holes. Wang *et al* [4] used a trapezoidal cavity placed at the back of the MPP to modify the coupling between the MPP and cavity. In such a configuration, the modes which are initially decoupled to the MPP in a rectangular backing cavity are now coupled. Thus, the original poor absorption region at the spectral dip was improved due to the coupling variation. The aforementioned studies, however, were mainly focused on the normal incidence case. In Maa [1], an approximate formula for the oblique incidence was proposed based on the path difference between incident wave and the reflective wave, for an infinite backing cavity. Thus,

influences from the modes which are predominately moving parallel to the MPP surface are neglected. The current work focuses on a cavity of finite dimension with a baffled MPP surface. The Patch Transfer Function (PTF) approach[5] is used to calculate the surface pressure of the MPP which makes it possible to consider an oblique incidence impinging on the MPP.

2. Theoretical modeling

The system under investigation is illustrated in Fig.1, which is composed of a MPP panel backed by a trapezoidal cavity having a inclined backing wall with a varying angle γ. Assuming an incident wave p_{in} impinging on the MPP with an incident angle of θ and azimuthal angle of β, the pressure outside of the cavity is $2p_{in}+p_{rad}$, where p_{rad} is the radiated sound pressure by the vibration of the MPP and the air particle velocity surrounding the MPP surface. Together with the sound pressure inside the cavity, p_{cav}, the sound pressure difference between the two sides of MPP generates the air mass vibration at each single hole. As the diameter of the hole is much smaller than the acoustic wavelength of interests, it is appropriate to assume that the air particle velocity is distributed uniformly within the area of each hole. Thus, the air particle velocity at the centre of the hole is governed by:

$$Z_{i,resist}\left[u_0 - u_p\right] + Z_{i,react}u_0 = \frac{1}{\rho_0 c}\left[p_{cav} - \left(2p_{in} + p_{rad}\right)\right], \tag{1}$$

where $Z_{i,resist}$ and $Z_{i,react}$ are the resistance and reactance of the relative specific acoustic impedance of the orifice hole Z_i (divided by $\rho_0 c$), respectively, u_0 is the particle velocity at the hole; u_p the vibration velocity of the flexible MPP. The explicit impedance expression for the MPP holes can be found in [1]. For an oblique plane wave impinging on the MPP, the incident wave is

$$\begin{aligned} p_{in} &= p_i e^{i(\omega t - k_x x - k_y y - k_z z)} \\ &= p_i e^{i(\omega t - k\sin\theta\sin\beta x - k\cos\theta y - k\sin\theta\cos\beta z)} \end{aligned}$$

where k_x, k_y and k_z are the wavenumbers in the x, y and z direction, respectively, p_i is the amplitude of the incident pressure.

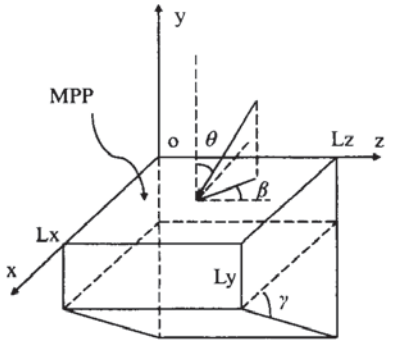

Figure 1 Schematic of a MPP absorber excited by an oblique incidence.

For a flexible panel, the governing equation for the vibration of the MPP itself is

$$D_p\nabla^4 w(x,z,t) + \rho_p\frac{\partial^2 w(x,z,t)}{\partial t^2} = p_{cav} - \left(2p_{in} + p_{rad}\right), \tag{2}$$

where D_p is the MPP's flexural rigidity; ρ_p the MPP surface density; w the normal panel displacement.

For a simply-supported boundary condition, the panel displacement w in harmonic regime is

$$w(x,z,t) = \sum_{i,j=1}^{IJ} A_{ij}\sin\left(i\pi x / L_x\right)\sin\left(j\pi z / L_z\right)e^{i\omega t},$$

where A_{ij} is the ijth modal amplitude; L_x and L_z the side lengths of the panel. The vibration velocity is

$$u_p(x,z,t)=\frac{\partial w(x,z,t)}{\partial t}=\sum_{ij=1}^{IJ} i\omega A_{ij}\sin(i\pi x/L_x)\sin(j\pi z/L_z)e^{i\omega t}. \tag{3}$$

For a stationary response analysis, the time dependence term is omitted in the following part. The air particle velocity u_0 is a series of discrete variable at each orifice. It is more convenient to describe the air motion u_0 in a spatially averaged sense as

$$\overline{u}_0=\sigma u_0.$$

where σ is the perforation ratio in percentage. Following the standard Galerkin procedure [6], the particle velocity over the MPP surface $\overline{u}_0$ is expanded as a series of sine functions,

$$\overline{u}_0(x,z)=\sum_{i,j=1}^{IJ} u_{ij}\sin(i\pi x/L_x)\sin(j\pi z/L_z), \tag{4}$$

where u_{ij} is the complex amplitude. With a proper truncation of the decomposition series, Eq. (4) could represent the averaged particle velocity field $\overline{u}_0$ accurately except at the boundary edges, which is shown to be negligible in the present vibro-acoustic analysis.
p_{cav} can be expressed in terms of acoustic modes of the rigid-walled cavity [7] as follows:

$$\begin{aligned} p_{cav}(x,y,z)&=\sum_{m,n=0}^{MN} A_{mn}\psi_{mn}(x,y,z)=\sum_{m,n=0}^{MN} A_{mn}\psi_m(x,y)\cos\frac{n\pi z}{L_z}\\ &=-\frac{i\rho_0 c^2\omega}{V}\sum_{m,n=0}^{MN}\frac{\psi_m(x,y)\cos\frac{n\pi z}{L_z}}{\Lambda_{mn}(\omega^2-\omega_{mn}^2)}\int_0^{L_x}\int_0^{L_z}\overline{u}_a(x',z')\psi_m(x',0)\cos\frac{n\pi z'}{L_z}dx'dz' \end{aligned} \tag{5}$$

where $\psi_m(x, y)$ is the mth acoustic mode of the cavity in the x-y plane; n the modal index in the z direction; A_{mn} the unknown modal amplitude for each cavity mode; V the cavity volume; Λ_{mn} the generalized acoustic mass of the mnth cavity mode; and $\overline{u}_a$ the surrounding air particle velocity in the vicinity of MPP which is defined as:

$$\overline{u}_a=(1-\sigma)u_p+\overline{u}_0. \tag{6}$$

For a MPP absorber inserted in an infinite baffle, the surface pressure can be calculated by the Patch Transfer Function (PTF) approach [5]. In this method, the panel is discretized into small patches and each patch vibrates like a monopole source. The radiation pressure at each patch is thereby contributed by two parts: first, the pressure radiated by the patch itself; and second, contribution from the other patches. Therefore, the radiation impedance is defined as

$$\begin{aligned} Z_{rr}&=\frac{\langle p_{rad}\rangle_r}{\langle\overline{u}_a\rangle_r}=\rho_0 c\left[1-e^{-\mathrm{j}ka}\right],\\ Z_{rs}&=\frac{\langle p_{rad}\rangle_r}{\langle\overline{u}_a\rangle_s}=\frac{1}{2\pi}\mathrm{j}\rho_0\omega\frac{e^{-\mathrm{j}kd_{rs}}}{d_{rs}}S_s. \end{aligned} \tag{7}$$

where r and s are the patch index; $k = \omega/c$ which is the wave number; S_s the surface area of the patch s and a the radius of a circular patch S_r.
Since Eq. (1) and (2) are a couple of equations with the unknown variables u_{ij} and A_{ij}, and the pressure term p_{rad} and p_{cav} are also expressed in terms of surrounding air particle velocity $\overline{u}_a$, the whole set of equations can be solved provided a sufficient number of modes is considered. Note the model developed here is also available for the irregular

shaped cavity in which case the eigenfunctions of the cavity should be obtained numerically. The sound absorption coefficient of the MPP absorber can be calculated as

$$\alpha_{\theta,\beta} = \frac{\rho_0 c \int_0^{L_x}\int_0^{L_z} \mathrm{Re}\left[p_e^* \cdot \overline{u}_a(x,0,z)\right] dxdz}{|p_i|^2 L_x L_z}. \tag{8}$$

where $p_e = 2p_{in}+p_{rad}$ and the asterisk denotes the complex conjugate.
For diffused incidence,

$$\overline{\alpha} = \int_0^{2\pi}\left(\int_0^{\pi/2} \alpha_{\theta,\beta} \sin 2\theta d\theta\right) d\beta. \tag{9}$$

3. Simulation

In order to validate the present model, a MPP with a large dimension cavity (20m * 20m) is used to compare with Maa's oblique incidence formula. The aim of using the large scale cavity is to avoid the effect caused by the modes which are moving parallel to the MPP surface. For a proper comparison, a rectangular cavity ($\gamma = 0°$) is used in the analysis to be consistent with Maa's case. Moreover, the clearly identified mode shapes are helpful in investigating the underlying coupling mechanism. For the sake of convenience, the vibration of the panel is excluded in the following numerical simulations.

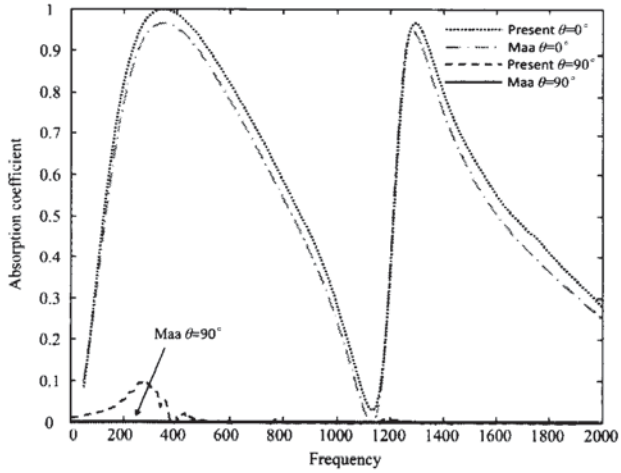

Figure 2 Comparison of the present model with Maa's formula at two different incident angles. $\theta = 0°$ & $\theta = 90°$ (Maa's formula for $\theta = 90°$ is a straight line lying on the horizontal axis).

Maa's model for oblique incidence with a cavity depth of 0.15m is used as a benchmark for comparison in two cases, i.e. $\theta = 0°$ & $\theta = 90°$. At $\theta = 0°$, the present model follows a same trend as Maa's curve, the small discrepancy maybe caused by the constraint of finite cavity size used in our simulation. For $\theta = 90°$, Maa's formula predicts zero absorption over the whole frequency spectrum. This is indeed the case, as for a grazing incidence, the cavity modes which are moving parallel to the MPP surface do not exist. Therefore, the MPP is totally decoupled from the backing volume which is of infinite length in Maa's configuration. The present model results in a very low absorption at the lower frequency range due to the limited volume size of the backing cavity. At higher frequencies, the absorption is nearly zero, in agreement with Maa's prediction. It can be further demonstrated that, if the dimension of the panel further enlarges, the absorption peak observed at low frequency range will shift to the lower frequency with a reducing amplitude (not shown in the current figure).

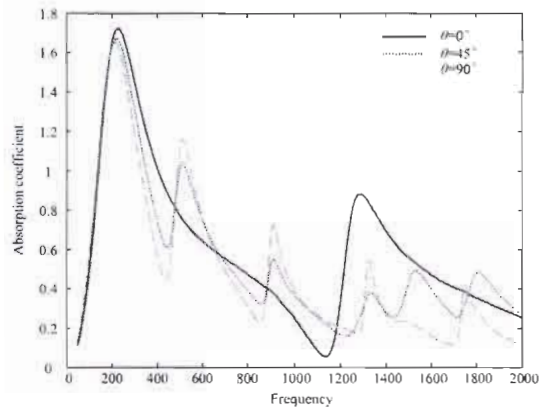

(a)

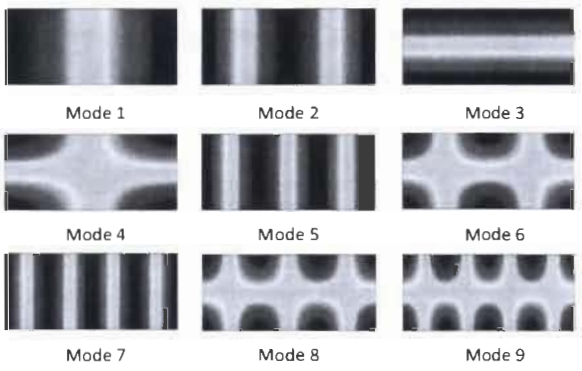

(b)

Figure 3 (a) Sound absorption coefficients with respect to different incident angles. (b) First 9 acoustic modes of the cavity (excludes the zero mode).

A MPP absorber subject to oblique incidence is numerically studied for a finite dimension cavity (Lx = 0.4m, Ly = 0.15m, Lz = 0.3m, γ = 0°), whilst the azimuthal angle β was kept constant at 90°. Three incident angles θ = 0°, 45° and 90° were considered, respectively. The sound absorption coefficients with respect to different angles are shown in Fig. 3(a). For the normal incidence (θ = 0°), two peaks are found. These peaks are actually induced by the non-grazing modes [4] (cf. the first 9 acoustic mode shapes of the cavity in Fig. 3(b)), as these modes dominate in the control of the sound absorption at the peaks. The MPP has a strong coupling with the non-grazing modes and these modes in turn dominate the sound absorption. Thus, at the frequencies where the non-grazing modes dominate, high absorption performance achieves. If the incident angle varies to 45°, the first peak does not change too much as it is mainly controlled by the air stiffness of the cavity. The second peak, however, is significantly suppressed. Furthermore, more ripples appear in the spectrum. If the incidence angle turns to 90° (termed as grazing incidence), a serial of new peaks are observed within the whole spectrum at 510 Hz, 910 Hz, 1330 Hz and 1750 Hz.

Based on our previous work for a normal incidence wave [4], a pair of specific absorption features, i.e. dip and peak, is a result of the coupling between the MPP and the non-grazing cavity modes. More peaks appearing in the spectrum indicates a coupling change of the system.

To demonstrate the coupling mechanism, two extreme cases, i.e. θ = 0° and θ = 90°, are investigated. Four frequencies corresponding to the peaks and dips at the two oblique angles are examined. Figure 4 illustrates the contribution of the first 10 cavity modes toward the total sound field in the backing cavity at these selected frequencies. For the normal incidence (first row), except the zero mode, the non-grazing type mode has a great contribution to the sound field. When θ = 90°, the grazing modes start to play an important role. Particularly, at the frequencies near the resonance of the 1st mode (first two columns in second row), its contribution is predominant. Similarly, at the frequencies close to the

resonance of the 3rd mode (last two columns in first row), it has a superior contribution than other modes.

Figure 4 Modal amplitude of the first 20 modes observed at different frequencies and incident angles. (a) 440 Hz, $\theta = 0°$; (b) 510 Hz, $\theta = 0°$; (c) 1140 Hz, $\theta = 0°$; (d) 1280 Hz, $\theta = 0°$; (e) 440 Hz, $\theta = 90°$; (f) 510 Hz, $\theta = 90°$; (g) 1140 Hz, $\theta = 90°$; (h) 1280 Hz, $\theta = 90°$. ■ grazing mode; ▤ non-grazing mode, □ other mode.

The waterfall plots of the sound absorption against different incident angles are presented in Fig. 5(a). The spectral peaks at 90° gradually vanish when the incidence varies from the grazing incidence to the normal incidence. This again indicates the coupling strength variation between the MPP and the cavity. From 90° to 0°, the dominant role of grazing mode decreases and the non-grazing mode becomes stronger in the absorption. Therefore, except for the first absorption peak, only the peak which is induced by the 3rd mode (non-grazing mode) is found in the spectrum at 0° incident angle.

It is expected that, for the diffuse incidence, different angles would result in multiple modal domination in the sound absorption. The coupling of either the grazing or non-grazing with the incidence at their strong coupling angles would cause more absorption peaks in the spectrum. This can be seen in Fig. 5(b), in which $\bar{\alpha}$ was calculated according to Eq. (9), whilst keeping $\beta = 90°$ for simplicity. In a sense, this is a 2-D diffused field results. Such a treatment is not the limitation of the present model but it avoids introducing too many modes which may complicate the understanding of the underlying physics. Indeed, more absorption peaks are observed in the spectrum. However, at the frequency where no effective coupling takes place, which means neither the grazing modes nor the non-grazing modes are well coupled to the MPP covering the whole angle variation, a big trough will be found. For example, at around 1200 Hz, the absorption performance is relative poor. This can be improved by using a trapezoidal cavity as shown in dashed curves, which indicates the potential of using trapezoidal backed cavity to alter the performance of the MPP at strategic frequency bands toward the objective of a broadband absorption.

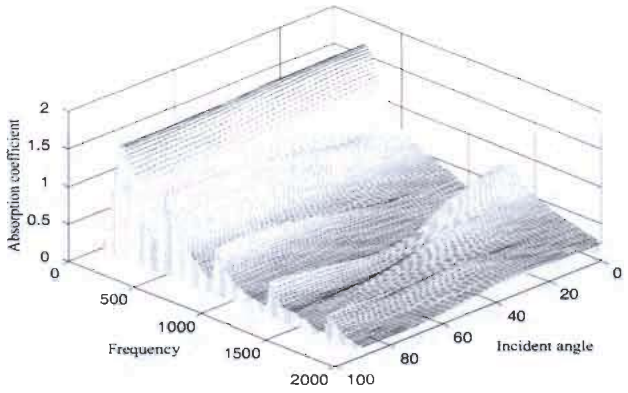

(a)

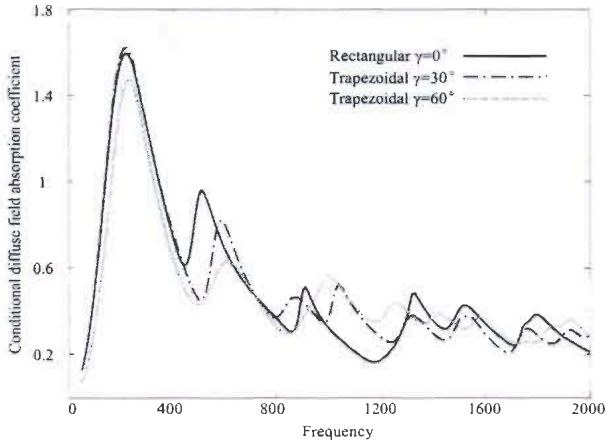

(b)

Figure 5 (a) Waterfall plot for the sound absorption of a MPP with rectangular cavity at different incident angle, (b) diffuse field sound absorption coefficient with three cavity configurations.

4. Conclusions

A model used to predict the absorption performance of the MPP backed by a cavity is developed in the current work. The use of PTF method to obtain the MPP surface pressure enables the analysis of an oblique incidence impinging on the MPP inserted in an infinite baffle. The model was validated through comparison with Maa's formula for the oblique incidence case using a backing cavity of a very large dimension. For the grazing incidence case, a noticeable absorption still exists at low frequency due to the effect of the air stiffness of the finite volume. Unlike the normal incidence case, a grazing incidence is more likely to excite the grazing modes, causing peaks and dips around the their corresponding resonances. Therefore, the use of a backing cavity of finite size can provide appreciate sound absorption at all incident angles. It was demonstrated that, incident angle will alter the coupling between the MPP and the backing volume, causing variation in the sound absorption curve. This alteration to the system coupling is further accentuated by the use of irregular-shaped cavity such as a trapezoidal one. This phenomenon can be explored to strategically change the cavity shape to optimize the sound absorption performance of the absorber in the desired frequency range.

References

(1) Maa D. Y., Theory and design of microperforated-panel sound-absorbing construction, Sci. Sin. Vol. XVIII, 55-71, 1975.
(2) Li Y. Y., Lee E. W. M., and Ng C. F., Sound absorption of a finite flexible micro-perforated panel backed by an air cavity, J. Sound Vib., 287 227-243 (2005).
(3) Sakagami K., Morimoto M., Yairi M., and Minemura A., A pilot study on improving the absorptivity of a thick microperforated panel absorber, Appl. Acoust. 69 179-182 (2008).
(4) Wang C. Q., Cheng L., Pan J., and Yu G. H., Sound absorption of a micro-perforated panel backed by an irregular-shaped cavity, J. Acoust. Soc. Am. 127 (1) 3313-3321 (2010).
(5) Chazot J., Guyader J., Prediction of transmission loss of double panels with a patch-mobility method, J. Acoust. Soc. Am. 121 (1) 267-278 (2007).
(6) Meirovitch L., Fundamentals of Vibrations, McGraw-Hill, Boston, 2001.
(7) Cheng L., Li Y. Y., and Gao J. X., Energy transmission in a mechanically-linked double-wall structure coupled to an acoustic enclosure, J. Acoust. Soc. Am. 117 (5) 2742-2751 (2005).

Acknowledgements

The authors wish to acknowledge support given to them by the Research Grants Council of HKSAR through Grant No. PolyU 5140/09E